Parametrization of Mean Radiative Properties of Optically Thin Steady-State Plasmas and Applications

R. Rodriguez[1,2,*], G. Espinosa[1], J. M. Gil[1,2], J. G. Rubiano[1,2],
M. A. Mendoza[1,2], P. Martel[1,2] and E. Minguez[2]

[1] *Departmento de Fisica, Universidad de Las Palmas de Gran Canaria, 35017, Spain.*
[2] *Instituto de Fusion Nuclear,Universidad Politecnica de Madrid, 28006, Madrid, Spain.*

Abstract. Plasma radiative properties play a pivotal role both in nuclear fusion and astrophysics. They are essential to analyze and explain experiments or observations and also in radiative-hydrodynamics simulations. Their computation requires the generation of large atomic databases and the calculation, by solving a set of rate equations, of a huge number of atomic level populations in wide ranges of plasma conditions. These facts make that, for example, radiative-hydrodynamics in-line simulations be almost infeasible. This has lead to develop analytical expressions based on the parametrization of radiative properties. However, most of them are accurate only for coronal or local thermodynamic equilibrium. In this work we present a code for the parametrization of plasma radiative properties of mono-component plasmas, in terms of plasma density and temperature, such as radiative power loss, the Planck and Rosseland mean opacities and the average ionization, which is valid for steady-state optically thin plasmas in wide ranges of plasma densities and temperatures. Furthermore, we also present some applications of this parametrization such as the analysis of the optical depth and radiative character of plasmas, the use to perform diagnostics of the electron temperature, the determination of mean radiative properties for multicomponent plasmas and the analysis of radiative cooling instabilities in some kind of experiments on high-energy density laboratory astrophysics. Finally, to ease the use of the code for the parametrization, this one has been integrated in a user interface and brief comments about it are presented.

---

*Corresponding author. *Email address:* `rafael.rodriguezperez@ulpgc.es` (R. Rodriguez)

1 Introduction

The role of the plasma radiative properties is known to be of decisive importance to many research fields at plasma physics such as astrophysics, X-ray laser development, laboratory plasma astrophysics, EUV lithography and inertial and magnetic confinement fusion, since they are essential to explain the experiments and the observations. Thus, for example, the opacities are fundamental in the design of hohlraum walls and the radiative power losses play an important role in the current decays after disruptions in magnetic nuclear fusion devices in which disruptions are assumed to be caused by strongly radiating impurities [1]. Furthermore, the data on mean or mean-group opacities and radiative power losses are required in radiative-hydrodynamics simulations and the monochromatic opacities and emissivities are used for plasma spectroscopic diagnostics. Therefore, it is essential to obtain sufficiently accurate data on plasma radiative properties within a wide range of plasma densities and temperatures.

The calculation of the plasma radiative properties implies the computation of the population of the atomic levels in the plasma. At high densities, where the plasma can be considered under local thermodynamic equilibrium (LTE) they can be obtained by means of the Saha-Boltzmann's equation. Also, in the low density regime, where Coronal equilibrium (CE) could be assumed, these quantities can be obtained using the simple equations of the CE model. However, these limit situations are exceptions and non-LTE (NLTE) conditions are commonly found in both laboratory and astrophysical plasmas. In NLTE the calculation of the plasma atomic level populations, and therefore of the radiative properties, shows great complexity because there is not a priori expression for these quantities and one must find them using the so-called collisional-radiative models (CRM) in which one has to solve a set of rate equations, as many as the number of atomic levels included in the model, with coupling of atomic configurations, free electrons and photons. Furthermore, CRMs reproduce, in stationary state, CE and LTE results at the extreme limits of low and high densities, respectively. Taking into account that accurate calculations of both atomic level populations and radiative properties entail to consider in the CRM as many levels as possible, the resolution of the resulting large system of rate equations becomes sometimes unmanageable and approximations must be made. For this reason, the theory of NLTE plasmas is a still very active subject and many NLTE codes have been developed [2–13] since the early proposals [14,15]. The complexity and the computational time cost of the resolution of CRMs has led to develop analytical expressions for the radiative properties in order to provide them in a fast way for in-line radiation-hydrodynamics. However, most of them are accurate only for CE [16–21] since they are density independent or for the range of high photon energies in LTE [22,23], but not for NLTE situations.

In this work we first present a method to parametrize the radiative power losses (RPL), Planck and Rosseland mean opacities and average ionizations, in terms of the density and temperature of the plasma, for steady-state optically thin mono-component plasmas. The databases of these quantities subject to the parametrization are calculated

by means of a CRM and, therefore, NLTE, LTE and CE regimes are covered. Secondly, we present some applications of their parametrization such as the analysis of the optical depth and the radiative character of plasmas, in obtaining the radiative properties of multi-component plasmas, the diagnosis of the electron temperature and the analysis and prediction of the onset of radiative cooling instabilities in radiative shocks in laboratory plasmas. With these purposes we have developed a computational tool called PARPRA, which is integrated on an user interface to ease its use.

The remainder of the paper is organized as follows: In Section 2 we briefly describe the CRM employed in this work to generate the databases of the radiative properties. In Section 3 we present the method developed for the parametrization of the radiative properties of mono-component plasmas and the computational code in which it is implemented. Sections 4 and 5 are devoted to the analysis of the application of the fittings to obtain radiative properties of plasma mixtures and to predict the onset of radiative cooling instabilities in some kind of experiments on high-energy density laboratory astrophysics, respectively. In the last section main conclusions are presented.

2 Generation of the databases of plasma radiative properties

The calculation of plasma radiative properties requires two previous steps. The first one is the calculation of the atomic data such as energy levels, transitions energies or oscillator strengths needed by the CRM. In this work those atomic data are obtained using FAC code [24] under the relativistic detailed configuration accounting (RDCA) approach. The radiative transitions rates in FAC are calculated in the single multipole approximation, and in this work they were obtained in the electric dipole approach. The Unresolved Transition Array (UTA) [25] formalism is used for the bound-bound transitions, so the transition energies include the UTA shift, and the width for each transition is considered. Furthermore, the line strengths are corrected for configuration interaction within the same non-relativistic configurations. As it is known the DCA approach can introduce inaccuracies in the calculation of the radiative properties of low Z elements. However, in this work we are interested in the procedure to fit those properties, and not so much in the atomic model employed to generate the atomic data, although the parametrization presented here can be also used for more detailed atomic descriptions.

The continuum lowering (CL) due to the influence of the plasma surrounding is also considered and is calculated by means of the expression due to Stewart and Pyatt [26] but using the particular proposal given in [27],

$$\Delta I_\zeta = \frac{3}{2} \frac{I_H a_0}{R_\zeta} (\zeta+1) \left\{ \left[1 + \left(\frac{D}{R_\zeta} \right)^3 \right]^{2/3} - \left(\frac{D}{R_\zeta} \right)^2 \right\}. \tag{2.1}$$

Here I_H is the Rydberg constant, a_0 is the Bohr radius, $R_\zeta = [3(\zeta+1)/(4\pi n_e)]^{1/3}$ is the ion-sphere radius assuming the plasma composed of ions with charge ζ only, the Debye

radius is $D = \left[4\pi\left(\overline{Z} + \overline{Z^2}\right)n_{ion}/T_e\right]^{-1/2}$, $\overline{Z}$ is the plasma average ionization, $\overline{Z^2}$ is the second order moment of the population distribution, n_{ion} and n_e are the ion and electron particle densities, respectively, and T_e is the electron temperature (assuming ion-electron thermalization).

The second step is to obtain the atomic level populations. In this work they were obtained using the CRM for steady-state situations (CRSS) implemented in ABAKO code [28]. Following the standard NLTE modeling approach, a rate equation system describing the population density of the atomic states is built and solved, giving the population distribution. Therefore, to find the level population distribution, under stationary situations, the following system of rate equations is solved

$$\sum_{\zeta' j} N_{\zeta' j} \mathbb{R}^+_{\zeta' j \to \zeta i} - \sum_{\zeta' j} N_{\zeta i} \mathbb{R}^-_{\zeta i \to \zeta' j} = 0, \tag{2.2}$$

where $N_{\zeta i}$ is the population density of the atomic level i of the ion with charge state ζ. The terms $\mathbb{R}^+_{\zeta' j \to \zeta i}$ and $\mathbb{R}^-_{\zeta' j \to \zeta i}$ take into account all the atomic processes (collisional and radiative) which contribute to populate and depopulate the state ζi, respectively. The processes included in the CR model are the following: collisional ionization [29] and three-body recombination, spontaneous decay, collisional excitation [30] and deexcitation, radiative recombination [31], electron capture and autoionization [32]. We have added between brackets the references from which their approximated analytical rates coefficients have been taken. This set of equations constitutes the so-called CRSS model. In ABAKO it is assumed that the system has had enough time to thermalize and, therefore, both the electrons and ions have a Maxwell-Boltzmann type energy distribution. Furthermore, in ABAKO it is also assumed that electron and ion temperatures are equal. Therefore, in the following, it will denote the plasma temperature by the electron temperature T_e.

Two complementary equations which have to be satisfied together with (2.2) are, first, the requirement that the sum of all the partial densities equals the total ion density, n_{ion},

$$\sum_{\zeta=0}^{Z} \sum_{i=0}^{M_\zeta - 1} N_{\zeta i} = n_{ion}, \tag{2.3}$$

and, second, the charge neutrality condition in the plasma,

$$\sum_{\zeta=0}^{Z} \sum_{i=0}^{M_\zeta - 1} \zeta N_{\zeta i} = n_e, \tag{2.4}$$

where M_ζ is the total number of levels for the charge state ζ. The plasma average ionization is defined as

$$\overline{Z} = \frac{\sum_{\zeta=0}^{Z} \zeta N_\zeta}{\sum_{\zeta=0}^{Z} N_\zeta} = \frac{n_e}{n_{ion}}. \tag{2.5}$$

When the CL correction is included the kinetics rate equations must be solved iteratively, since the atomic data depend on ionization balance by means of $\overline{Z}$ and $\overline{Z^2}$. A more detailed description of the CRSS model implemented in ABAKO can be found in [28].

Once the atomic data and the atomic level populations are available, the plasma radiative properties can be calculated. In this work we are interested in the parametrization of Planck and Rosseland mean opacities and in the RPL and they were calculated using RAPCAL code [33,34] which was coupled to ABAKO code [35]. The mean opacities are obtained from the monochromatic absorption coefficient, denoted in this work as $\kappa(\nu)$, and it includes the bound-bound, bound-free and free-free contributions

$$\kappa(\nu) = \kappa_{bb}(\nu) + \kappa_{bf}(\nu) + \kappa_{ff}(\nu), \tag{2.6}$$

where ν is the photon frequency. The bound-bound contribution to the absorption is given by

$$\kappa_{bb}(\nu) = \sum_{\zeta} \sum_{i,j} \kappa_{\zeta i \to \zeta j}(\nu), \tag{2.7}$$

with

$$\kappa_{\zeta i \to \zeta j}(\nu) = \frac{h\nu}{4\pi} N_{\zeta i} \frac{g_{\zeta j}}{g_{\zeta i}} \frac{c^2}{2h\nu_{ij}^3} A_{\zeta j \to \zeta i} \phi_{ij}(\nu) \left(1 - \frac{g_{\zeta i}}{g_{\zeta j}} \frac{N_{\zeta j}}{N_{\zeta i}} \right), \tag{2.8}$$

where c is the speed of light, $g_{\zeta i}$ and $g_{\zeta j}$ are the statistical weights of the i and j levels, respectively, $A_{\zeta j \to \zeta i}$ is the Einstein coefficient for spontaneous deexcitation between the bound states j,i of the ion ζ and h is the Planck's constant. In the previous equation, $\phi_{ij}(\nu)$ represents the line profile for line absorption. In the evaluation of the line profile, natural, Doppler, UTA and electron-impact [36] broadenings were included. The line-shape function is applied with the Voigt profile that incorporates all these broadenings.

The bound-free contribution to the absorption is given by

$$\kappa_{bf}(\nu) = \sum_{\zeta,i} \sum_{\zeta,j} \kappa_{\zeta i \to \zeta+1j}(\nu), \tag{2.9}$$

with

$$\kappa_{\zeta i \to \zeta+1j}(\nu) = N_{\zeta i} \sigma_{\zeta i \to \zeta+1j}^{pho}(\nu) \left(1 - \frac{N_{\zeta+1j} n_e f(\varepsilon)}{N_{\zeta i}} \frac{g_{\zeta i}}{g_{\zeta+1j} g(\varepsilon)} \right), \tag{2.10}$$

with ε the energy of the free electron and m_e the electron mass. $g(\varepsilon)$ is the density of states with energy ε which, assuming an ideal gas of free electrons, is given by

$$g(\varepsilon) = 4\pi \left(\frac{2m_e}{h^2} \right)^{3/2} \varepsilon^{1/2}. \tag{2.11}$$

A Maxwell-Boltzmann distribution, $f(\varepsilon)$, is assumed at temperature T_e for the free electrons. The photoionization cross section, $\sigma_{\zeta i \to \zeta+1j}^{pho}(\nu)$, has been evaluated in this work using the semiclassical expression of Kramers [31].

For the free-free contribution to the absorption the Kramers semi-classical expression for the inverse bremsstrahlung cross section has been used [37], which is given by

$$\kappa_{ff}(\nu) = \frac{16\pi^2 e^2 h^2 \alpha}{3\sqrt{3}(2\pi m_e)^{3/2}} \frac{\overline{Z^2} n_{ion} n_e}{T_e^{1/2}(h\nu)^3} \left(1 - e^{-h\nu/T_e}\right),$$ (2.12)

where α is the fine-structure constant. In order to determine the opacity, $k(\nu)$, it is also taken into account the absorption due to the scattering of photons. In RAPCAL this one is approximated using the Thomson scattering cross section [38]

$$\kappa_{scatt} = n_e \sigma^{Thom},$$ (2.13)

with $\sigma^{Thom} = 6.65 \times 10^{-25}$ cm^2. Finally, the opacity is given by

$$k(\nu) = \frac{1}{\rho} \left(\kappa(\nu) + \kappa_{scatt}\right),$$ (2.14)

Therefore, Planck k_P and Rosseland k_R mean opacities are given by [39]

$$k_P = \int_0^\infty d\nu \tilde{B}(\nu, T_e)(k(\nu) - \kappa_{scatt}/\rho),$$ (2.15)

$$\frac{1}{k_R} = \int_0^\infty d\nu \frac{\partial \tilde{B}(\nu, T_e)}{\partial T_e} \frac{1}{k(\nu)},$$ (2.16)

where $\tilde{B}(\nu, T)$ is the normalized Planckian function,

$$\tilde{B}(\nu, T_e) = \frac{15}{\pi^4 T_e} \frac{u^3}{e^u - 1}, \quad u = \frac{h\nu}{T_e}.$$ (2.17)

The RPL is evaluated as following [40] in (eV/s/ion). For the bound-bound contribution

$$P_{bb} = \sum_\zeta \sum_{ij} h\nu_{ij} A_{ij} N_{\zeta j}.$$ (2.18)

The bound-free contribution is given by

$$P_{bf} = 4\pi \sum_\zeta \sum_{ij} N_{\zeta i} \left(\frac{N_{\zeta+1j} N_\zeta}{N_{\zeta i} N_{\zeta+1}}\right)^{LTE} \int_{\nu_0}^\infty \sigma_{\zeta i \to \zeta+1j}^{pho}(\nu) \left(\frac{2h\nu^3}{c^2}\right) e^{-h\nu/T_e} d\nu,$$ (2.19)

where ν_0 is the threshold energy for each bound-free transition and the LTE population ratio is obtained from Saha equation. The contribution from the free-free transitions is given for a pure Coulomb field in (eV/s/ion) as following [41]

$$P_{ff} = 9.55 \times 10^{-14} n_e T_e^{1/2} \sum_\zeta Z_\zeta^2 N_\zeta,$$ (2.20)

where it has been assumed the gaunt factor equal to unity. The total radiative power loss is then obtained as the sum of the three contributions.

For the parametrization, the databases of the average ionization, the mean opacities and the RPL were calculated using ABAKO/RAPCAL in logarithmic meshes of densities and electron temperatures in the range of plasma conditions in which we were interested in.

3   Parametrization of the radiative properties of mono-component plasmas

Once we have generated the databases of the radiative properties we can proceed to their parametrization. Due to the nature of these properties we have observed that, from a numerical point of view, it is more convenient to perform a parametrization of the decimal logarithm of the property than of the property itself. Therefore, if A denotes the radiative property to parametrize, the analytical expression employed for the fitting is the following

$$\log A(d,T_e) = \sum_{i=0}^{n}\sum_{j=0}^{m} C_{ij}(\log d)^i (\log T_e)^j, \tag{3.1}$$

where d denotes either the electron particle density, the ion particle density or the density of matter. The coefficients of the fitting, C_{ij}, are determined by means of a Least Square Regression. If we denote as $x = \log d$ and $y = \log T_e$, the polynomial used for the fitting has the following expression

$$P(x,y) = \sum_{i=0}^{n}\sum_{j=0}^{m} C_{ij} x^i y^j. \tag{3.2}$$

If we denote by n_x and n_y the number of points of densities and temperatures, respectively, of the database, the coefficients will be obtained through the minimization of the following function

$$F(C_{ij}) = \sum_{k=1}^{n_x}\sum_{l=1}^{n_y} \left(P(x_k,y_l) - D_{kl}\right)^2, \tag{3.3}$$

where D_{kl} is the radiative property evaluated at density 10^{x_k} and temperature 10^{y_l} of the database. Then, from the equation for the minimization

$$\frac{\partial F(C_{ij})}{\partial C_{ij}} = 0, \tag{3.4}$$

it is obtained a set of $(n+1)\cdot(m+1)$ coupled algebraic equations

$$\sum_{k=1}^{n_x}\sum_{l=1}^{n_y}\sum_{i=0}^{n}\sum_{j=0}^{m} C_{ij} x_k^{i+q} y_l^{j+r} = \sum_{k=1}^{n_x}\sum_{l=1}^{n_y} D_{kl} x_k^q y_l^r, \quad q=0,\cdots,n;\; r=0,\cdots,m. \tag{3.5}$$

Polynomials of high degree can be highly oscillatory and therefore they can provide values of the radiative properties for plasma conditions that do not belong to the mesh used for the parametrization very different with the ones calculated with the CRSS model. We have observed that, for the properties that we are analyzing, this fact can be avoid fixing the maximum degree of the polynomial both in electron temperature, m, and density, n, to 7. Then, the procedure to obtain the coefficients of the polynomial fitting is the following: starting from the lower polynomial degree the coefficients are obtained

solving the set of equations (3.5). Then the value obtained from the fitting is compared to the calculated one. If the relative difference is lower than a criterion imposed then the procedures finishes. Otherwise, the polynomial degree is progressively increased until the criterion is fulfilled. However, it could happen that the maximum degree of the polynomial is reached but the criterion is not fulfilled. Therefore the range of densities and temperatures must be divided into sub-ranges to obtain a polynomial fitting in each one of them and then to repeat the same procedure. In our parametrization, in order to optimize this division, a quad-tree algorithm is used, which is a tree data structure often used to partition a two dimensional space (density and temperature, in this case) by recursively subdividing it into four regions. Finally, we will obtain as many polynomial functions as divisions of the whole range of plasma conditions under analysis. The final number of divisions will depend on the margin of error imposed in the parametrization. Obviously, as the error becomes more restrictive, the number of divisions, and, therefore, of polynomial functions, obtained increases. As an example, we present in Table 1 the number of polynomial functions obtained for the fitting of the cooling rate, which is obtained as the ratio of the RPL and the electron and ion particle densities, of a carbon plasma for a range of electron densities $10^{12}-10^{20}$ cm^{-3} and of electron temperatures of 1-1000 eV. The maximum relative error imposed in the fitting was 10%. The number of divisions, and therefore of polynomials functions, obtained in the fitting was 10. In the table are listed the average relative errors obtained either in points that belong or not to the database used for the fitting, for each one of the divisions.

Table 1: Number of the division and average relative errors in each one of them for either points that belong or not to the database for the fitting of the cooling rate of a carbon plasma with a maximum relative error imposed of 10%.

Number	Database (%)	Non-database (%)
1	1.93	2.41
2	2.45	3.05
3	3.64	3.65
4	1.46	2.16
5	4.12	4.01
6	1.24	2.40
7	3.34	3.71
8	3.4	4.52
9	2.18	2.38
10	2.54	3.68

From Table 1 it is observed that in general the average relative error is larger for points that do not belong to the database as it is expected. Fig. 1 shows a comparison between the fitting of the cooling rate and its numerical calculation as a function of the electron temperature and for three electron densities. From the figure it is observed the good agreement of the fitting.
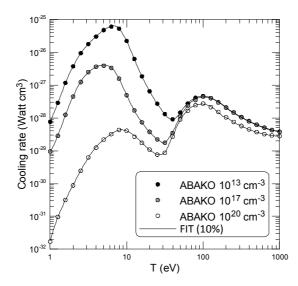
Figure 1: Parametrization of the cooling rates of a carbon plasma assuming a relative error of 10%.

As it was commented previously, there are available in the literature fittings of the average ionization and cooling rates [16–21] that are widely used. However, they were obtained in the context of CE, (low density regime) and they are density independent. But, even at low density regime, these fittings should be used carefully since CE approach is not accurate for the whole range of temperatures. Thus, for example, for carbon plasmas we have detected that CE is an accurate approach for electron densities lower than 10^{15} cm^{-3} provided that the electron temperature was greater than 30 eV [42]. On the other hand, there are also analytical fittings of the mean opacities [22,23], but they are accurate for high photon energies only and they were obtained under LTE assumption. However, the parametrization proposed in this work depends on both density and temperature and it is valid for CE, LTE and NLTE and it has been already used in the parametrization of the average ionization and cooling rates of carbon plasmas in a wide range of plasma conditions [42] and for the average ionization, RPL and mean opacities for krypton and xenon plasmas in a range of plasma conditions of interest in some laboratory astrophysics experiments [51].

A straightforward application of the parametrization of Planck mean opacities and RPL of mono-component plasmas is related to the field of laboratory astrophysics in which astrophysical phenomena are properly recreated at laboratory scale. The popularity of this field has grown considerably mainly due to two factors: the demonstration that the hydrodynamics can be scaled correctly between laboratory and astrophysics scenarios [43] and, second, the improvement of high-power laser systems that allow us to generate plasmas that are in regimes for certain astrophysical systems. Those laboratory experiments not only permit to explain and predict what occurs in astrophysical phenomena but also provide important data for validation and verification of several aspects of numerical codes such as atomic physics, equation of state, radiative transfer and

hydrodynamics, that are employed in other topics in the field of plasma physics. One of the most interesting astrophysical phenomena is the radiative shock wave, which is a shock wave where the radiation transport is important to the total energy budget. Then, the shock wave is radiatively driven so that its dynamics can be significantly modified by radiative processes. Since radiative shocks are ubiquitous throughout the universe, their simulations in laboratory using gases is currently a research area of interest [44–47]. In these kind of experiments two things must be addressed: the first one is to characterize the optical depth of the plasma in which the shock wave is propagating, both in the shocked and unshocked plasma regions. The second one is to establish the radiative character of the shock. For both aspects these parameterizations of the radiative properties have demonstrated their utility. According to Ryutov et al. [43] for the radiative shock to be optically thin the mean free path of the photons in the plasma, $\overline{\lambda}_{rad}$, calculated as

$$\overline{\lambda}_{rad} = \frac{1}{\rho \overline{\kappa}_P}, \tag{3.6}$$

must be larger than a characteristic size, h, of the system. On the other hand, for the radiative shock to be radiative, according to [43], the radiative cooling time, t_{cool}, must be shorter than the convective transport time, $t_{conv} = h/s$, where s is the plasma sound speed. The radiative cooling time is given by

$$t_{cool} = 2.42 \times 10^{-12} \frac{(\overline{Z}+1)n_{ion}T_e}{-\nabla \cdot \vec{F}_{rad}}, \tag{3.7}$$

where $\vec{F}_{rad}$ is the radiative flux and its divergence, if the radiation energy does not depend explicitly on time, is given by

$$-\nabla \cdot \vec{F}_{rad} = \int_0^\infty j(\nu)d\nu - \int_0^\infty \kappa(\nu)I(\nu)d\nu, \tag{3.8}$$

where $I(\nu)$ is the specific intensity of the radiation. For simplicity we have omitted in the previous equations the dependence of these magnitudes on time, position and propagation direction, although they depend on them. If the cooling time is much smaller than the convective transport time then the plasma can be considered as radiative. The first addend on the right side of (3.8) is the RPL. If the plasma is optically thin then the second addend on the right hand can be neglected and therefore the divergence of the radiative flux is the RPL. On the other hand, when the plasma is optically thick it is common to approach this second addend by the Planck mean opacity. Hence, both in optically thin and thick situations, the parametrization of the RPL and the Planck mean opacity will allow us to calculate the photon mean free path and the cooling time for a wide range of plasma conditions in a fast and accurate way and, in fact, we have already employed these fittings in [48] to characterize blast waves (an expanding shock that is in the process of sweeping up the material that is ahead of the shock) launched in xenon clusters

using the THOR laser system at the University of Texas [47] generated to reproduce and analyze the ones produced in supernova remnants.

The polynomial fitting of the average ionization in terms of the density and electron temperature can be used in some experiments to perform a diagnosis of the electron temperature. If the plasma densities and the average ionizations are known from the experiment the electron temperatures diagnosed will be those that, for each density, provide from the polynomial fitting an average ionization that matches with the experimental one within a margin of error imposed. In particular, we have already applied it in Rodriguez et al. [48] to diagnose the electron temperatures of the blast waves launched in xenon clusters before commented entailing an error lower than 0.1% in the diagnosis. Furthermore, the fitting of the average ionization is very useful since it appears in the calculation of many relevant coefficients involved in hydrodynamics simulations such as the ions mean free paths, electron collision frequency, specific plasma conductivity, kinematic viscosity and the coefficient of heat conduction [49], for example.

The algorithm for the parametrization as well as the handling of the databases of the radiative properties to fit and also the subsequent applications of these fittings have been recently integrated in a computational code developed with that purpose named PARPRA. Furthermore, in order to simplify its use, PARPRA is integrated in a graphic user interface that also allows the user to generate several graphical representations of the properties fitted.

4   Mean radiative properties for multi-component plasmas

As it is known, multi-component plasmas are very common in both astrophysics and nuclear fusion, and, therefore, their radiative properties are needed as well. Obviously, if the determination of radiative properties for mono-component plasmas entails large computational costs, these ones grow when the plasma is a mixture of different elements. Using PARPRA we are able to obtain the average ionization, the Planck mean opacity and the RPL of the plasma mixture from their parametrization for the individual components in terms of the electron density and temperature. This method is accurate if any atomic process that connect different elements in the plasma is not included. Since we are dealing with optically thin plasmas the coupling through the radiative transfer is neglected. On the other hand, in the CRSS implemented in ABAKO collisional processes between two different elements in the plasma are not included. Since the plasma consists of ions of different elements immersed into a sea free electrons the components of the plasma mixture are coupled through the electron density, since the average ionization of each element has to be consistent with the same electron density, which ensures the electrical equilibrium keeping the overall plasma neutrality. The method proposed to obtain the mean radiative properties of the multicomponent plasma from the individual ones is based on that fact. On the other hand, the elements in the plasma could be also coupled through the CL, since in (2.1) the average ionization is the one of the mixture. However,

when the parametrization of the radiative properties of the individual elements is made, the average ionization is the corresponding one to the element only. Therefore, this fact could introduce some inaccuracies in the method. Obviously, the discrepancies will be significant when two conditions are fulfilled: first, that the average ionization of the mixture is very different from the average ionization of some of the elements of the plasma and, second, that in the plasma conditions the CL is important, i.e at high densities and moderate and low temperatures. This item will be analyzed thereafter.

Our procedure to obtain the radiative properties of the mixture depends on which is the type of density known for the mixture, i.e. electron number density, ion number density or density of matter. In the first case the procedure is very simple since we just have to evaluate the fittings of the individual elements for the electron density and temperature of the mixture. Then, the radiative property of the mixture is evaluated by adding the property of each element weighted by its fractional abundance. If the input is the ion number density we have to made an iterative procedure in order to obtain the electron density of the mixture and then its radiative properties. This starts assuming that the initial electron density for the mixture is equal to the ion density and then we proceed as in the first case. Then a new set of average ionizations of the individual elements is obtained. With this set the average ionization of the mixture is evaluated and a new electron density and we proceed, again, as in the first case. This process continues until the average ionization of each individual element varies no more than a set tolerance from the previous self-consistent iteration. Eventually, we obtain the average ionization of the mixture and its electron density which allows us to obtain the RPL and the Planck mean opacity from the individual fittings.

Table 2 presents a comparison of the average ionization and RPL for a plasma of two components, Ne and Ar, between the calculations made using the CRSS model implemented in ABAKO and the ones obtained from the parametrization carried out in PARPRA. In the parametrization of the radiative properties of the individual components a relative error of 0.1% was imposed. We have selected two cases of low temperature, 3 eV, and electron densities of 10^{16} cm^{-3} and 10^{20} cm^{-3}(cases 1 and 2 in the table, respectively) in order to analyze the possible discrepancies that can arise due to the CL, since for the former electron density the effect of CL is negligible but for the latter one we have observed the influence of the CL in the calculation of the average ionization. It is observed that the increasing of the density and, therefore, of the relevance of the CL, does not introduce any additional discrepancy with respect to the lower density cases. We can also observe that the relative differences between CRSS and PARPRA calculations decrease for the case 3 with respect to cases 1 and 2. This is due to the fact that the plasma condition of the former is one of those considered in the databases of the individual components fitted but not in the latter cases. This fact, as it was shown in Table 1, justifies the lower difference.

Furthermore, we have also analyzed the influence of the iterative procedure implemented in PARPRA for multi-component plasmas in which the ion particle density is known but not the electron density, see cases 4 and 5. In these cases the convergence cri-

Table 2: Comparisons of the average ionization and RPL between the calculations carried out using the CRSS (CR) model and PARPRA (PA) for a mixture of Ne and Ar. The fractional abundance of Ne is 0.7. The temperatures are given in eV, the particle densities in cm^{-3} and the RPL in erg/s/cm^3.

	T_e	n_e	n_{ion}	$\overline{Z}^{PA}$	$\overline{Z}^{CR}$	RPL^{PA}	RPL^{CR}
Case 1	3	10^{16}	−	1.479	1.412	3.96×10^{11}	4.86×10^{11}
Case 2	3	10^{20}	−	0.228	0.229	1.75×10^{17}	1.86×10^{17}
Case 3	40	10^{20}	−	7.741	7.715	5.29×10^{18}	5.34×10^{18}
Case 4	5	−	10^{16}	2.365	2.379	1.56×10^{13}	1.60×10^{13}
Case 5	5	−	10^{18}	2.274	2.254	8.85×10^{15}	8.87×10^{15}

Table 3: Comparisons of the average ionization and RPL between the calculations carried out using the CRSS (CR) model and PARPRA (PA) for a mixture of Ne, Ar, Al and Xe. The fractional abundances are 0.25 for each component. The temperatures are given in eV, the particle densities in cm^{-3} and the RPL in erg/s/cm^3.

	T_e	n_e	n_{ion}	$\overline{Z}^{PA}$	$\overline{Z}^{CR}$	RPL^{PA}	RPL^{CR}
Case 1	3	10^{16}	−	2.418	2.312	1.55×10^{12}	1.75×10^{12}
Case 2	3	10^{19}	−	1.395	1.310	2.12×10^{16}	1.90×10^{16}
Case 3	20	10^{19}	−	7.061	7.020	7.66×10^{17}	6.10×10^{17}
Case 4	20	−	10^{16}	6.327	6.323	2.96×10^{14}	2.83×10^{14}
Case 5	20	−	10^{19}	6.689	6.714	1.68×10^{19}	7.25×10^{18}

terion in the self-consistent procedure in the average ionization was 0.1%. From the table it is observed that this procedure does not introduce more noticeable differences. These results have been checked analyzing other multicomponent plasmas.

In Table 3 we present a comparison similar to the one shown in Table 2 but for multicomponent plasma compounded of four elements: Ne, Ar, Al y Ne in order to check if the method proposed is more inaccurate as the number of components in the plasma increases. However, it is clear from the table that the relative differences between both calculations are of the same order as those obtained for the plasma of two components. Therefore, the number of components of the plasma and the iterative procedure due to the ion density does not seem to introduce noticeable discrepancies between both calculations (CRSS and PARPRA) as it can be observed in Tables 2 and 3. The main source of differences between both calculations is that the plasma condition analyzed belongs or not to the ones considered in the databases of the radiative properties fitted of the individual components.

Finally, the input can be the density of matter of the multicomponent plasma and the mass fractions of the elements. As in the case of the ion particle density, the objective is to find the electron density of the mixture. Therefore, the first step is to transform the density of matter of the multicomponent plasma to the ion density. For this purpose in PARPRA we assume that the components of the plasma are ideal gases and then each one

of them will have a partial pressure, following Dalton's law, and then a partial density given by

$$\rho_i = m_i \rho_M, \tag{4.1}$$

where m_i if the mass fraction of the component i. Since the partial densities are additive we have

$$\sum_{i=1}^{N} \rho_i = \rho_M. \tag{4.2}$$

Thus, the starting ion density will be given by

$$n_{ion} = N_A \rho \sum_{i=1}^{N} \frac{m_i}{A_i}, \tag{4.3}$$

where N_A is Avogadro's number and A_i is the atomic weight of the element i. After that, the procedure would be the same as the one for the ion density case commented above.

We would like to point out that although the starting point of the iterative process in this case is the assumption of ideal gases for the components of the plasma, this fact does not limit its application to low density and temperature plasmas (the range in which the ideal gas approach is more appropriate) since the self-consistent procedure is carried out in the electron density of the multicomponent plasma as in the case of the ion particle density. Therefore, the components in the plasma interact through the common free electron gas and then the ideal gas approach, in which the components do not disturb or interact with each other, is no longer assumed. Thus, when the self-consistent is achieved and the iterative method finishes, the average ionization of each component in the plasma is consistent with the same electronic density. According to Klapisch et al. [50] this fact ensures the electrical equilibrium and the chemical equilibrium is achieved as a consequence and, moreover, the method is thermodynamically consistent. In that paper the authors find the electron density of the multicomponent plasma assigning a partial volume to each element and solving the following equation

$$\sum_{i=1}^{N} \frac{m_i}{\rho_i(n_e)} - \frac{1}{\rho} = 0, \tag{4.4}$$

and they conclude that this method provides accurate radiative properties of multicomponent plasmas from their individual components. We have made a comparison of our method with the one proposed in [50] in order to show that both methods provide the same results. In particular, we have selected a plasma of four components (Ne, Ar, Al and Xe) with the same mass abundances (0.25). In Table 4 we show the average ionizations of each one of the four elements and the average ionization and the RPL of the mixture for four plasma electron temperatures and matter densities, calculated using the equation of Klapisch et al. [50]. We also present in the table the electron densities of the mixture obtained for each plasma condition. In Table 5 we present the same but obtained with the iterative procedure implemented in PARPRA. The agreement obtained both in

Table 4: Electron density and average ionizations of each of the four components and of the mixture and the total RPL obtained using (4.4). The temperatures are given in eV, the matter densities in gcm^{-3}, the electron densities in cm^{-3} and the RPL in erg/s/cm^3.

	T_e	ρ	n_e	$\overline{Z}_{Ne}$	$\overline{Z}_{Al}$	$\overline{Z}_{Ar}$	$\overline{Z}_{Xe}$	$\overline{Z}_{Mix}$	RPL$_{Mix}$
Case 1	2	10^5	2.32×10^{17}	0.852	1.902	1.109	1.803	1.293	3.564×10^{13}
Case 2	10	10^{-5}	7.26×10^{17}	3.367	3.180	5.667	7.354	4.046	5.352×10^{15}
Case 3	20	10^{-5}	1.09×10^{18}	5.442	5.028	7.792	9.405	6.060	1.286×10^{16}
Case 4	20	10^{-4}	1.11×10^{19}	5.560	5.160	7.752	9.766	6.164	3.963×10^{17}

Table 5: Average ionizations of each of the components and of the mixture and the RPL obtained using the iterative method implemented in PARPRA. The RPL is given in erg/s/cm^3.

	$\overline{Z}_{Ne}$	$\overline{Z}_{Al}$	$\overline{Z}_{Ar}$	$\overline{Z}_{Xe}$	$\overline{Z}_{Mix}$	RPL$_{Mix}$
Case 1	0.852	1.902	1.109	1.800	1.293	3.579×10^{13}
Case 2	3.367	3.177	5.667	7.365	4.046	5.351×10^{15}
Case 3	5.442	5.030	7.792	9.379	6.058	1.287×10^{16}
Case 4	5.551	5.156	7.748	9.762	6.158	3.963×10^{17}

Table 6: Average ionizations of each of the components and of the mixture and the RPL obtained using the CRSS model of ABAKO. The RPL is given in erg/s/cm^3.

	$\overline{Z}_{Ne}$	$\overline{Z}_{Al}$	$\overline{Z}_{Ar}$	$\overline{Z}_{Xe}$	$\overline{Z}_{Mix}$	RPL$_{Mix}$
Case 1	0.849	1.846	1.109	1.806	1.270	3.800×10^{13}
Case 2	3.369	3.178	5.665	7.397	4.034	5.285×10^{15}
Case 3	5.441	4.981	7.793	9.376	6.029	1.221×10^{16}
Case 4	5.590	5.080	7.746	9.796	6.137	3.412×10^{17}

the average ionizations and in the RPL between both methods is excellent, as it can be seen from the tables. In Table 5 we have omitted the resulting electron densities since they are practically the same than the ones presented in Table 4. The fact of having the polynomial fittings of the radiative properties of the individual components provides us an advantage respect to other models based on databases, as for example in [50], because it avoids any interpolation procedure from the databases.

We have also made a comparison with calculations carried out using the CRSS model implemented in ABAKO. In this case we have employed as plasma conditions the electron temperatures and the electron densities presented in Table 4. In Table 6 we present the results. From the comparisons we observe that both our method and the one proposed in [50] show a very good agreement with the ones provided by the CRSS model.

4.1 Analysis of thermal instabilities

Instabilities that occur due to a balance between heating and cooling rates in the plasma are described as thermal cooling instabilities. The subject of thermal cooling instabilities has attracted a lot of attention over the last four decades [52–56] in reference to formation of stars and planets, and it has been also shown to produce stable oscillations in radiative shock front oscillations [54]. The possibility of the onset of the thermal cooling instability is studied in terms of the scaling of the RPL [57–62]. This one is scaled in a power law in the form $RPL \propto \rho^\alpha T_e^\beta$. This expression is included in the hydrodynamic equations to take into account the energy losses through radiation. Then, a stability analysis is made in order to establish the values of the parameters, α and β, that would lead to the thermal instability. Therefore, it is necessary to perform the power law parametrization of the RPL and for this purpose the polynomial fitting presented in this work is very useful. Imposing the equality between the polynomial function and the power law, and their first derivatives respect to the temperature and density, we would obtain the coefficients α and β in terms of the coefficients of the fitting for each plasma condition

$$\alpha = \frac{\sum_{i=1}^{n}\sum_{j=0}^{m} i C_{ij} x^i y^j}{\sum_{i=0}^{n}\sum_{j=0}^{m} C_{ij} x^i y^j}, \tag{4.5}$$

$$\beta = \frac{\sum_{i=0}^{n}\sum_{j=1}^{m} j C_{ij} x^i y^j}{\sum_{i=0}^{n}\sum_{j=0}^{m} C_{ij} x^i y^j}. \tag{4.6}$$

We have already applied this method to analyze the possibility of the onset of thermal cooling instabilities in the blast waves previously commented launched both in krypton and xenon gases [51]. In particular, in that case α was fixed to 2, which is a common approach when the main contribution to the RPL is the bremsstrahlung, and although in those experiments this is not true, in Rodriguez et al. [51] it was checked that the approach was locally still valid. For $\alpha = 2$ the shock is expected to be susceptible to the thermal cooling instability if β is lower than 0.8 [59, 60]. In that work the polynomial fitting of the RPL of both krypton and xenon was used to determine the parameter β in the range of plasma conditions of the experiment, and this allowed us to determine the range of temperatures in which the instability should be observed in the blast waves launched in krypton and to conclude that for xenon in order to detect it the temperatures required should be higher than the ones reached in the experiments, and this fact implies the need of irradiating the cluster with more powerful lasers [51]. These conclusions agreed with the experimental observations.

5 Conclusions

In this work we have presented a parametrization of mean radiative properties of mono-component steady-state plasmas such as Rosseland and Planck mean opacities, the ra-

diative power loss and the plasma average ionization. This parametrization has the advantage with respect to others available in the literature that depends on both the plasma density and temperature. Furthermore, the databases of the radiative properties subject to the fitting can be generated using a CRSS model and therefore CE, LTE and NLTE regimes can be reproduced. These facts bring an improvement with respect to other fittings available in the bibliography. These parameterizations are very useful to perform in-line radiative-hydrodynamic simulations since they provide in a fast an accurate way the needed properties and coefficients for each plasma condition in the simulation. We have presented some straightforward applications of these fittings such as obtaining of the cooling time and the photon mean free path of a plasma, the calculation of the radiative properties of multicomponent plasmas from the fittings of the properties of the individual components and the analysis of the onset of thermal cooling instabilities in radiative shocks. Both the parametrization and its applications have been developed in a computational code named PARPRA which is integrated in a user interface to ease its use. It is our future aim to continue improving and increasing the capabilities of PARPRA introducing new applications of the parameterizations in order to provide a useful tool for the user.

Acknowledgments

References

[1] T. Pinna and L.C. Cadwallader, Component failure rate data base for fusion applications, Fusion Eng. Des., 51-52 (2000), 579-585.
[2] A. Bar-Shalom, J. Oreg and M. Klapisch, Recent developments in the SCROLL model, J. Quant. Spectrosc. Radiat. Transfer, 65 (2000), 43-55.
[3] O. Peyrusse, A superconfiguration model for broadband spectroscopy of non-LTE plasmas, J. Phys. B: At. Mol. Opt. Phys., 33 (2000), 4303-4321.
[4] A. Bar-Shalom, M. Klapisch and J. Oreg, HULLAC, an integrated computer package for atomic processes in plasmas, J. Quant. Spectrosc. Radiat. Transfer, 77 (2001), 169-188.
[5] Yu. V. Ralchenko and Y. Maron, Accelerated recombination due to resonant deexcitation of metastable states,J. Quant. Spectrosc. Radiat. Transfer, 71 (2001), 609-621.
[6] G. Faussurier, C. Blancard and E. Berthier, Nonlocal thermodynamic equilibrium self-consistent average-atom for plasma physics, Phys. Rev. E, 63 (2001), 026401.
[7] S.B. Hansen, Development and application of L-shell spectroscopic modeling for plasma diagnostics, Ph.D. Thesis, University of Nevada, (2003).
[8] J. Bauche, C. Bauche-Arnoult and K.B. Fournier, Model for computing superconfiguration temperatures in non-local-thermodynamic-equilibrium hot plasmas, Phys. Rev. E, 69 (2004), 026403.

 [9] H. K. Chung, M. H. Chen, W. L. Morgan, Y. Ralchenko and R. W. Lee, FLYCHK: Generalized population kinetics and spectral model for rapid spectroscopic analysis for all elements, High Energy Density Phys., 1 (2005), 3-12.
[10] C.J. Fontes, J. Colgan, H.L. Zhang and J. Abdallah Jr., Large-scale kinetics modeling of non-LTE plasmas, J. Quant. Spectrosc. Radiat. Transfer, 99 (2006), 175-185.
[11] J. Q. Pang, Z. Q. Wu and J. Yan, Emissivity calculations under DCA-UTA approximation for NLTE plasmas, Commun, Comput. Phys., 2 (2007), 1085-1094.
[12] C. Gao, J. Zeng, Y. Li, F. Jin and J. Yuan, Versatile code DLAYZ for investigating population kinetics and radiative properties of plasmas in non-local thermodynamic equilibrium, High Energy Density Phys., 9 (2013), 583-593.
[13] Y. Frank, E. Louzon, P. Mandelbaum and Z. HenisSEMILLAC: A new hybrid atomic model of hot dense plasmas, High Energy Density Phys., 9 (2013), 594-600.
[14] D. R. Bates, A. E. Kingston and R.W. P.McWirther, Recombination between electrons and atomic ions. I. Optically thin plasmas, Proc. R. Soc. London, Ser. A, 267 (1962),297-312.
[15] R. W. P. McWhirther, Data needs, priorities and accuracies for plasma spectroscopy, Phys. Rep., 37 (1978), 165-209.
[16] D.E. Post, R.V. Jensen, C.B. Tarter, W.H. Grasberger, and W.A. Lokke, Steady-state radiative cooling rates for low density, high-temperature plasmas, Atom. Data Nucl. Data, 20 (1977), 397-439.
[17] H.P. Summers and R.W.P. McWhirter, Radiativ epower loss from laboratory and astrophysical plasmas. I. Power loss from plasmas in steady-state ionisation balance, J. Phys. B: Atom. Mol. Phys., 12 (1979) 387-411.
[18] K.B. Fournier, D. Pacella, M.J. May, M. Finkenthal and W.H. Golstein, Calculation of the radiative cooling coefficient for molybdenum in a low density plasma, Nucl. Fusion, 37 (1997), 825-834.
[19] K.B. Fournier, M.Cohen, M.J. May and W.H. Goldstein, Ionization state distribution and radiative cooling rate for argon in a low density plasma, Atom. Data Nucl. Data, 70 (1998), 231-254.
[20] K.B. Fournier, M.J. May, D. Pacella, M. Finkenthel, B.C. Gregory and W.H. Goldstein, Calculation of the radiative cooling coefficient for krypton in a low density plasma, Nucl. Fusion, 40 (2000), 847-863.
[21] K.M. Schure, D. Kosenko, J.S. Kaastra, R. Keppens and J. Vink, A new radiative cooling curve based on an up-to-date plasma emission code, Astron. Astrophys. 508 (2009), 751-U240.
[22] E. Minguez, R. Ruiz, P. Martel, J.M. Gil, J.G. Rubiano, R. Rodriguez, Scaling law of radiative opacities for ICF elements, Nucl. Instrum Meth A, 464 (2001), 218-224.
[23] E. Minguez, P. Martel, J.M. Gil, J.G. Rubiano, R. Rodriguez, Analytical opacity formulas for ICF elements, Fusion Eng. Des., 60 (2002), 17-25.
[24] M.F. Gu. The flexible atomic code, Can. J. Phys., 86 (2008), 675-689.
[25] J. Bauche, C. Bauche-Arnoult, M. Klapisch, Transition arrays in the spectra of ionized atoms, Adv. At. Mol. Phys., 23 (1987), 131-195.
[26] J.C. Stewart, K.D. Pyatt. Lowering of ionization potentials in plasmas, Astrophys. J., 144 (1966), 1203-1211.
[27] R. M. More, Atomic physics in inertial confinement fusion, Technical Report UCRL-84991, Lawrence Livermore National Laboratory, 1981.
[28] R. Florido, R. Rodriguez, J. M. Gil, J. G. Rubiano, P. Martel, E. Minguez and R. C. Mancini, Modeling of population kinetics of plasmas that are not in local thermodynamic equilibrium, using a versatile collisional-radiative model based on analytical rates, Phys. Rev. E, 80 (2009),

056402.

[29] W. Lotz, Electron-impact ionization cross sections and ionization coefficients for atoms and ions from hydrogen to calcium, Z. Phys. 216 (1968), 241-247.

[30] H. V. Van Regemorter, Rate of collisional excitation in stellar atmospheres, Astrophys. J. 136 (1962), 906-915.

[31] H. A. Kramers, On the theory of X-ray absorption and of the continuous X-ray spectrum, Philos. Mag. 46 (1923), 836-871.

[32] H. R. Griem, Principles of plasma spectroscopy, Cambridge University Press, 1997.

[33] R. Rodriguez, J.M. Gil, R. Florido, J.G. Rubiano, P. Martel, E. Minguez, Code to calculate optical properties for plasmas in a wide range of densities, J. Phys. IV, 133 (2006), 981-984.

[34] R. Rodriguez, R. Florido, J.M. Gil, J.G. Rubiano, P. Martel, E. Minguez, RAPCAL code: a computational package to compute radiative properties for optically thin and thick low and high-Z plasmas in a wide range of density and temperature, Laser Part. Beams, 26 (2008), 433-448.

[35] R. Rodriguez, R. Florido, J.M. Gil, J.G. Rubiano, D. Suarez, P. Martel, E. Minguez, R.C. Mancini RC, Collisional-Radiative calculations of optically thin and thick plasmas using the computational package ABAKO/RAPCAL. Commun. Comput. Phys., 8 (2010), 185-210.

[36] M. S. Dimitrijevic and N. Konjevic, Simple estimates for Stark-broadening of ion lines in stellar plasmas, Astron. & Astrophys., 172, (1987), 345-349.

[37] S.J. Rose, Calculations of the radiative opacity of laser-produced plasmas, J. Phys. B., 25 (1992), 1667-1681.

[38] R.J. Rutten, Radiative Transfer in Stellar Atmospheres, Utretch University Lectures Notes 8th Edition, 2003.

[39] F.J.D. Serduke, E. Minguez, S.J. Davidson, C.A. Iglesias, WorkOp-IV summary: lessons from iron opacities, J. Quant. Spectrosc. Radiat. Transf., 65 (2000), 527-541.

[40] H.K. Chung, K.B. Fournier, R.W. Lee, Non-LTE kinetics modeling of krypton ions: Calculations of radiative cooling coefficients, High Energy Density Phys., 2 (2006), 7-15.

[41] W.J. Karzas, R. Latter, Electron radiative transitions in a Coulomb field, Astrophys. J., 6 (1961), 167-212.

[42] J.M. Gil, R. Rodriguez, R. Florido, J.G. Rubiano, M.A. Mendoza, A. de la Nuez, G. Espinosa, P. Martel, E. Minguez, Parametrization of the average ionization and radiative cooling rates of carbon plasmas in a wide range of density and temperature, J. Quant. Spectrosc. Radiat. Transfer, 125 (2013), 123-138.

[43] D. Ryutov, R.P. Drake, B.A. Remington, Similarity criteria for the laboratory simulation of supernova hydrodynamics, Astrophys. J., 518 (1999), 821-832.

[44] B. Fryxell, E. Rutter, E.S. Myra, Simulations of laser experiments of radiative and non-radiative shocks, High energy Density Phys., 8 (2012), 141-149.

[45] E. Falize, A. Ravasio, B. Loupias, A. Diziere, C.D. Gregory, C. Michaut et al., High-energy density laboratory astrophysics studies of accretion shocks in magnetic cataclysmic variables, High energy Density Phys., 8 (2012), 1-4.

[46] A.D. Edens, T. Ditmire, J.F. Hansen, M.J. Edwards, R.G. Adams, P.K. Rambo et al., Measurement of the decay rate of single-frequency perturbation on blast waves, Phys. Rev. Lett., 95 (2005), 244503.

[47] J. Osterhoff, D.R. Symes, A.D. Edens, A.S. Moore, E. Hellewell, T. Ditmire, Radiative shell thinning in intense laser-driven blast waves, New J. Phys., 11 (2009), 023022.

[48] R. Rodriguez, G. Espinosa, J.M. Gil, R. Florido, J.G. Rubiano, M.A. Mendoza et al., Analysis of microscopic magnitudes of radiative blast waves launched in xenon clusters with

collisional-radiative steady-state simulations, J. Quant. Spectrosc. Radiat. Transfer, 125 (2013), 69-83.

[49] R.P. Drake, High-Energy-Density physics, Springer, 2005.

[50] M. Klapisch, M. Busquet, Models for the computation of opacity of mixtures, New J. Phys., 15 (2013), 015012.

[51] R. Rodriguez, J.M. Gil, G. Espinosa, R. Florido, J.G. Rubiano, M.A. Mendoza et al., Determination and analysis of plasma parameters for simulations of radiative blast waves launched in clusters of xenon and krypton, Plasma Phys. Control. Fusion, 54 (2012), 045012.

[52] G.B. Field, Thermal instability, Astrophys. J., 142 (1965), 531-567.

[53] J.H. Hunter, Jr., Thermal stability and its application to the interstellar gas, Astrophys. J., 161 (1970), 451-455.

[54] S.H. Langer, G. Chanmugam, G. Shaviv, Thermal instability in accretion flows onto degenerate stars, Astrophys. J. Lett., 245 (1981), L23-L26.

[55] D. Lynden-Bell, C.A. Tout, Russell lecture: Dark star formation and cooling instability, Astrophys. J. Lett., 558 (2001), 1-9.

[56] E. O. Vasiliev, Thermal instability in a collisionally cooled gas, Mon. Not. R. Astron. Soc., 419 (2012), 3641-3648.

[57] R.A. Chevalier, J.N. Imamura, Linear-analysis of an oscillatory instability of radiative shock-waves, Astrophys. J., 261 (1982), 543-549.

[58] J.N. Imamura, M. Wolff, R.H. Durisen, A numerical study of the stability of radiative shocks, Astrophys. J., 276 (1984), 667-676.

[59] P.A. Kimoto, D.F. Chernoff, Radiative instabilities in simulations of spherically symmetric supernova blast waves, Astrophys. J., 485 (1997), 274-284.

[60] J.M. Laming, Relationship between oscillatory thermal instability and dynamical thin-shell overstability, Phys. Rev. E, 70 (2004), 057402.

[61] B. Ramachandran, M.D. Smith, The influence of the Mach number on the stability of radiative shocks, Mon. Not. R. Astron. Soc. 366 (2006), 586-608.

[62] M. Hohenberger, D.R. Symes, J. Lazarus, H.W. Doyle, R.E. Carley, A.S. Moore et al., Observation of a velocity domain cooling instability in a radiative shock, Phys. Rev. Lett., 20 (2010), 205003.